Determining the mineral composition in quaternary sediments of Amazon River Fan through regression techniques, basic well logs and gamma ray spectrometry

Jefferson Falcão & Abel Carrasquilla, UENF – Macaé - RJ

Abstract

The geophysical well logging records physical properties of the subsurface rocks that are useful to the exploitation of oil and mineral reserves. Through the measurements of the physical properties made from basic geophysical logs, it is possible to infer information such as: density, porosity, shaliness, fluid type and saturation. More elaborate information about subsurface as: pictures, throat size of pores, and minerals can be acquired by application of advanced logs as, for example, the resistive and acoustical images, nuclear magnetic resonance and geochemical logs. This work uses advanced geochemical log for mineralogical analysis of wells from the Amazon Fan through data collected by 155 IODP (International Ocean Discovery Program) expedition. This analysis involves the generation of basic theoretical logs, using mineral oxides derived from geochemical logging as input. These synthetic logs are compared with actual basic logs by the Proportional Integral Derivative (PID) controller and through this comparison, mineral oxides volumes are set. In addition to the mineralogical fit, some applications with basic and advanced loggings are made in order to know the composition of the sediments in Amazon Fan, estimating parameters such as: shaliness, matrix, porosity and fluid through the basic logs, and rocks classification through the geochemical log data.

Introduction

Geophysical well logging is one of the methods widely used in the characterization of geological formations in teh subsurface (Desbrandes, 1985.). Some relevant information commonly obtained by the logs is: well diameter, layer thickness, porosity, density, argilosity, fluid types and lithology of the formations. The other more specific information is: size of the grains and pores, permeability and mineralogy (Serra, 1984).

In relation to mineralogy, this can be obtained by the application of the geochemical log (GLT). This tool is basically composed of the components of natural gamma ray detection (NGT), aluminum activation (AACT) and gamma ray spectrometry (GST). Together, they allow the detection of up to 10 elements. The spectrum energy of these gamma rays is analyzed and the concentration of some elements in the formation is obtained. This is achieved by the emission of high energy neutrons from an artificial source installed in the logging tool, which then interacts with the drilling hole, geological formations and drilling fluid (Crain, 2015).

The analysis of the mineralogical composition of the rocks, therefore, offers the possibility of a better geological characterization in the wells. Among its primary applications are the well-to-well correlation, grain size calculation, sandstone classification, thermal conductivity estimation, rock generation, among others. These logs are very useful in the evaluation of formations, for example the determination of clay volumes may be more accurate and, therefore, the estimation of the saturation of the fluids is also improved (Oord, 1991).

According to Debrabant et al. (1997), the Amazonian Fan is the third largest underwater fan in the modern oceans. It extends for about 700 km from the continental shelf, towards the sea, has an area of approximately 375000 km2 and a water depth of 1000 - 4300 m. Through it, a huge area of sinuous channels approximately 1200 km from the mouth of the Amazon River spreads radially (Pirmez et al., 1997). In it can be found large channel fluvial deposits, which are usually marked by the grain descending and decreasing the thickness of the sedimentary packages. These deposits originate from a very large sediment discharge from the Amazon River (Figure 1). Regarding these same authors clay - rich deposits, and high sedimentation rates often characterize large fans. In addition, the variation of the distribution of these clay minerals actually expresses successive stages of tectonic, climatic and eustatic events, which end up controlling the size of the fan (Oliveira, 2009).

In accord to Flood et al. (1995), the river carries a sediment load that corresponds to 10% of the fluvial sediments of the planet, which are discharged on the Amazonian Fan since the Andean uplift in the Miocene. This region has large sedimentary deposits that are true records of continental climate, ocean circulation and tectonic activities over time. Currently, sediments from the river do not reach beyond the continental shelf. This is because the sea level is high, but during the glacial period, when sea level was low, sediments were discharged directly into the underwater canyon (Rabinowitz et al., 1994).

This work has as main objective to analyze and apply regression techniques in basic logs and geochemical data (gamma ray induction geochemical) obtained from the Amazon River Fan, collected by the International Ocean Discovery Program (IODP). These regression techniques aim to adjust the compositions of mineral oxides of the Amazonian Fan. A computer program developed by Cae-

tano (2014) was adapted for this case study, including some specificities for the Amazonian Fan data.

Method

The data used in the simulations were taken from the expedition of drilling in the Amazon Fan (Leg 155), which drilled wells 931B, 933A, 935A, 936A, 940A, 944A and 946A. All these wells have the basic well logs (acoustic, density, neutron and natural gamma rays). Geochemical log data (GLT) were collected only at wells 931B and 936A at depths of 50-100 up to 250-300 m, with which we will work. The GLT tool used has the main elements capture modules: the compensated neutron module (CNT-G), the aluminum activation module (AACT) and finally the induced gamma ray spectrometry (GST) (Herron & Herron, 1996).

After the acquisition of geochemical data, it is necessary to process them to obtain the concentrations of the elements (Galford et al., 2009). For this, this IODP mission used a set of computational routines specific to the lithologies found at the study site. These routines mainly make the conversion of the relative spectral concentrations of the elements to fractions by weight of the oxides SiO_2, $CaCO_3$, Al_2O_3, FeO, K_2O and TiO_2 (oxides model) with their statistical errors (Ewert & Harvey, 1995).

To estimate the volume of the minerals that best adjusts the responses of simplified log derived from the real logs a code developed by Caetano (2014) was used. The system of equations that generate the logs is composed of 23 minerals and 3 fluids, which interactively fits the volume of each mineral, considering the first attempt of *a priori* geological information from the core and plugs, with the procedure stopping when a minimum error less than of 1% between the real and simulated logs is reached.

To accomplish this process, the PID control scheme was used, which joints proportional actions in time (P, depends on actual error, which minimizes the error), integral (I, accumulation of errors of the past, which resets the error) and derivative (D, forecasting future errors, which looking faster ahead the error). The PID control is currently the most widely used in industries, in procedures with a single input and output, in which there is only one controlled input variable and a monitored output variable. The weighted sum of the three actions is used to adjust the process via a control element; for example, fitting a function in the other (Johnson & Moradi, 2005).

The script to adjust the volume of minerals from such an initial attempt developed a routine that implements a set of equations that modifies the input variables (mineral volumes) that simulate the logs so that the values of the simulated log converge to the simplified log values of the studied lithology. Considering only the density log, adjusting the volume of the mineral through the PID is described by Equations 1, 2, 3 and 4, in which Equation 9 is the error that arises when considering the actual log ρ_{log} = SP, the fractional mineral volume V_i = CV and the simulated log ρ_s = PV. In that equation, SP, CV and PV are the input and the output of the PID controller process described as process setpoint, control and variable, respectively. In this case, we consider the error $E\rho = \rho_{log} - \rho_s$ and the influence of the mineral in the ρ_s response, which depends on V_i and the difference $\Delta m = \rho_m - \rho s$, where ρ_m is the density of the mineral, i.e., the difference between ρm and ρ_s, and the volume changes of this mineral will influence the change in the log. To adjust the volume of a mineral, only $E_{(t)}$ and Δm are considered, besides the change rate in error and the speed at which the error changes (Figure 4).

$$E_{\rho}^{n} = \left(\frac{\rho_{\log} - \rho_s^n}{\rho_{\log}} \right) \left(\frac{\rho_m - \rho_s^n}{\rho_s^n} \right), \quad (1)$$

$$\boldsymbol{E}_{(t)}^{n} = \boldsymbol{E}_{\rho}^{n} + \boldsymbol{E}_{GR}^{n} + \boldsymbol{E}_{\phi}^{n}, \quad (2)$$

and

$$V_i^n = k_p E_{(t)}^n + k_i \int E_{(t)}^n dt + k_d \frac{dE_{(t)}^n}{dt}, \quad (3)$$

or

$$V_i^n = V_i^{n-1} \left[1 + k_p \left(E_{(t)}^n - E_{(t)}^{n-1} \right) + k_i E_{(t)}^n + k_d \left(E_{(t)}^n - 2E_{(t)}^{n-1} - E_{(t)}^{n-2} \right) \right], \quad (4)$$

In the above equations:

- ρ, ϕ, and GR are the indexes corresponding to the density log, the porosity log and the GR log, respectively;
- n is the index for the step of fit ($V^0{}_i$ is the initial value of the mineral volume i);
- k_p is the constant proportional to the error;
- k_d is the constant proportional to the product (error vs time);
- k_i is the constant proportional to the rate of change of error.

The program that calculates the inverse modelling was also developed in Matlab (2014) and simulates the influence of each lithology at each wellbore log. For a given lithotype, the program employs a model rock-fluid, and from this model, it is observed how each individual constituent of a volume of rock affects the final response of the geophysical measurement (e.g., radioactivity, density). Conversely, based on the values of simplified logs (e.g., GR, RHOB, NPHI and DT), it is possible to obtain the fractional volume of the minerals that comprise the rock of the previous estimate (Caetano, 2014).

Results

Sedimentary rock classification through crossplots can be found in the literature, such as Herron (1988). This application was made for well 931B and the results are contained in Figure 2. To facilitate the study, well 931B was divided into three representation ranges: 96.8 - 115.5 m and 162.2 - 224.9 characterized by higher gamma radiation and 115.5 - 162.2 m for less radiation. These are related to the shaliness, and verified the mineralogical influences in these zones. In this figure, it is noticed that the points are in the majority in the shaliness interval, and far from the strip of the quartz that is shortly after the marking 1.5 of the abscissa axis. It is possible to notice that according to this classification few points are in the range that characterizes the great amount of iron oxide, being the data divided in the zone of clay, wacke, lithic sandstone and arcosian sandstone. In well 936A a division was made in two intervals 122 - 200 m with lower gamma radiation and 200 - 277 m with higher radiation, since this one presents more homogeneous characteris-

tics. These two bands are related to larger and smaller shaliness, which may be associated with different mineralogical characteristics. Figure 3 shows that the points are located in the clay band, similar to well 931B, which has a strong relation to the clay content. Especially the deeper band is furthest from the quartz zone.

For the inversion process, the volumes of each mineral, together with the fluids present in the pores, form the input data. With them, the initial response, considered theoretical, is calculated, which will be adjusted to the real logs through the PID algorithm presented in Equations 1-4. For convergence, we consider a maximum error of 15% in the difficult points and minor errors in the easy points.

The simulations for well 931B were performed in the range of 96.774 – 224.942 m, where entirely the basic and complete geochemical logs are present. Figure 3 presents the responses of the theoretical and real logs of gamma ray, resistivity, porosity, density and sonic. In this figure, we show that the theoretical gamma ray log has a smaller response when compared to the actual values at approximately 20 ° API. In this instance, being influenced mainly by potassium, but also by thorium and uranium. Nonetheless, potassium besides influencing the gamma ray log also has a significant influence on the other logs. Its volume is much higher when compared to thorium and uranium, which, despite influencing the radiation, have insignificant volumes to influence sonic logs and porosity. This lower response leads the algorithm to increase the volume of potassium oxide, in order to increase the response of this log, even more with a good fit with the real log. The resistivity log had its response influenced mainly by water and potassium oxide present in clay minerals in values between 2 and 10 ohm.m, where the adjustment was better. In this same figure, the neutron porosity log obtained a lower value when compared with the real log, more specifically where the values of radioactivity were higher. It can be noticed that when there are many oxides, the hydrogen is rarely counted, which causes a decrease of the neutron porosity, highly influenced by this element. It can also be observed that this log converged well for the real. This amount of hydrogen that would lack in the medium would be strongly related to the hydrated minerals, that is to say, that they have water in its composition, as is the case of some minerals of clay. This is confirmed that in the parts with greater shaliness the algorithm recalculates this volume, adding more water to compensate the low theoretical response of the neutron log. In relation to the porosities calculated from the theoretical density and sonic logs, it is also possible to observe a decrease in this property when it reaches zones with less shaliness. The real sonic log had high values and the log density values were low in relation to the simulated logs.

Figure 4 shows the results of the mineral content derived from the reverse process of fitting the actual well logs. The value that fit the silicon oxide was higher for a few points and its content was decreased mainly in the bands of greater shaliness. However, this decrease was not significantly high, around 5% in the points of greatest shaliness. Silicon oxide is found in its pure form in quartz grains, but in clay minerals such as kaolinite ($Al_2Si_2O_5(OH)_4$), for example, it is associated with aluminum oxide and water according to formula of oxides. These depths where they had their concentration of silicon removed can confirm the bearing of a large quantity of clay minerals, due to the inclusion of water in place of silicon and aluminum oxides. The iron and titanium oxides had a low influence in the mineral adjustment, since these elements occur in low quantity in the minerals present and likewise by their high specific masses and low neutron porosity response. Even so, it is possible to notice some points in which the fit took a much smaller amount compared to the other minerals. This is powerfully associated with their properties and input volumes. Potassium oxide had its adjustment greatly influenced by its radioactive properties. Despite its comparatively low volume fraction, it causes a significant influence on the gamma ray log, which generally runs a good reading in the well logs. Along with this, the water was another component with greater readjustment and this happened in the zones of greater shaliness.

In well 936A, the range containing all the basic and geochemical logs is in the depth of 122.24 - 277.23 m. The convergence criteria used in this case are the same as for well 931B. Figure 5 shows the responses of the theoretical and real logs of gamma ray, resistivity, porosity, density and sonic. This figure also shows that the theoretical gamma ray log in this well was also smaller than the actual response at approximately 20 ° API. Higher responses in real logs may be associated, among other factors, with potassium interference in the drilling mud. In this occasion, seawater contains a significant amount of this element, particularly in the form of the chloride, although this effect is corrected. The resistivity log, in general, was in the range of clayey rocks around 2 - 10 ohm.m. In the shallowest part of the studied section this log was shown to be less resistant, confirming a greater presence of water with more saline characteristic. Similarly to well 931B, the values of high argilosity strongly impacted the real neutron log so that their values were of the order of 40 pu. The adjusted value for this log was of the order of 8 pu, lower than the real neutron porosity one. This fit also impacted the other porosity logs. In the higher clayey range, the minerals are most hydrated and should be corrected for the inclusion of water. The porosity of the theoretical density log was eminent than that of the real log. This difference was most pronounced in the deepest part, where the density is higher and the water content is lower. As in well 931B, the actual sonic log had a very high measurement and it was possible to correct it by adjusting the minerals with the help of theoretical responses. This log had lower reading at the lower part evidenced by the shorter transit time, associated with a greater amount of matrix.

For well 936A, silicon oxide had a substantial diminution in the deeper and clayey zone, indicating a greater initial contribution in the shallower layers. In the deeper layers the substitution of this mineral was around 10% in volume, where it was compensated with the inclusion of potassium oxide and water (Figure 6). It may be noted that water, aluminum oxide and silicon have a greater influence with depth, which shows that they are more abundant in these strata. This has a direct influence on the density and neutron porosity logs, which shows that

the consideration of these two logs is important for the adjustment of the minerals components of the rocks. In the lower portion of the well, where calcium carbonate is present in large quantities, it was replaced in the order of 2% at the deepest points, being smaller in the lower zones. It can be seen from Figure 6 that the aluminum oxide had a small substitution with an upper limit of 5% in the deeper layers. In contrast, the potassium oxide had values practically constant throughout the depth, increasing its volume in the formation, where its adjustment influenced the log of gamma rays by the radioactive properties.

Conclusions

The aim of this work was the application of regression techniques of basic and advanced well logs for the adjustment of mineral compositions of the Amazonian Fan. This was done using real data of both basic and geochemical logs, this last obtained with the GLT tool, what made it possible. a better analysis in relation to the models adopted. With the data from wells 931B and 936A, drilled by IODP (International Ocean Discovery Program), it was possible to analyze the properties of the rocks as well as the geology of the site. This study was more detailed in the sections where the logs are complete, in this case the sum of basic logs with the advanced geochemical log was essential for the work, allowing the integrated analysis between these two. The program developed by Caetano (2014) for mineral fit was modified mainly to meet the simulation conditions of the studied area. Some of these modifications were: input parameters for simulation in large quantities of layers, inclusion of mineral oxide compositions and physical properties, new equations for gamma ray simulation, induction log, sonic log, new output parameters for plotting graphs and different convergence criteria. The simulations carried out emphasized the great influence of clay minerals, especially in the amounts of silicon, aluminum and water oxides. The latter had great influence in the simulations, since it appears in large quantities associated with these minerals, greatly impacting the neutron log and the fit of the minerals represented by the oxide fractions. It is hoped that this study could serve as a basis for a greater understanding and deepening, not only of the geological information on the site, as well as the improvement of the techniques of data processing of logs of this type.

Acknowledgments

We thank the UENF/LENEP computing infrastructure, as well as the FAPERJ scholarship master's degree.

References

- Caetano, L. 2014. Simulation of the influence of lithology on the well logs of the Namorado Oilfield in Campos Basin. Completion of Graduation Course Work, UENF/LENEP, Macaé, 136 p. (In Portuguese).
- Crain, R. 2015. Crain´s petrophysical handbook. Spectrum, 2000. Available in <http://www.spec2000.net>. Access: 22 nov.
- Debrabant, P.; Lopez, M. & Chamley, H. 1997. Clay mineral distribution and significance in quaternary sediments of the Amazon Fan. In: National Science Foundation. Proceedings, Ocean Drilling Program scientific results, p. 177–192.
- Desbrandes, R. 1985. Encyclopedia of well logging. Editions Ophrys, 618 p.
- Ewert, L. & Harvey, P. 2015. Leg 155: Geochemical Processing Report. 1995. Available in <http:-//brg.ldeo.columbia.edu/logdb/>. Acess: 30 nov. 2015.
- Flood, R.; Piper, D. & Klaus, A. 1995. Proc. ODP, Init. Repts., 155: College Station, TX (Ocean Drilling Program).
- Galford, J.; Quirein, J.; Shannon, S.; Truax, J. & Witk owsky, J. 2009. Field test results of a new neutron induced gamma-ray spectroscopy geochemical logging tool. Society of Petroleum Engineers, p. 22.
- Herron, M. 1988. Geochemical classification of terrigenous sands and shales from core or log data. Journal of Sedimentary Research, Society for Sedimentary Geology, v. 58, n. 5.
- Herron, S. & Herron, M. 1996. Quantitative lithology: an application for open and cased hole spectroscopy. Transactions of the SPWLA 37th Annual Logging Symposium, New Orleans, paper E.
- Johnson, M. & Moradi, M. 2005. PID control: new identification and design methods. Springer-Verlag London Limited, 558 p.
- Matlab. 2014. Online user´s manual.
- Oliveira, V. 2005. The gravitational tectonics in the Amazon Cone: structural subdivision and control mechanisms. Master Thesis, UFF, Niteroi, 98 p. (In Portuguese).
- Oord, R. 1991. Evaluation of geochemical logging. The Log Analyst, SPWLA, Houston, v. 32, n. 01, p. 23 – 35.
- Pirmez, C.; Flood, R.; Baptiste, J.; Yin, H. & Manley, P. 1997. Clay content, porosity, and velocity of Amazon Fan sediments determined from ODP Leg 155 Cores and wireline logs. Geophysical Research Letters, 24, 317 - 320.
- Rabinowitz, P.; Francis, T.; Baldauf, J.; Coyne, J.; Harding, B.; McPherson, R.; Merrill, R. & Olivas, R. 1994. Ocean drilling program: Results from ninth year of drilling operations. Offshore Technology Conference, p. 26.
- Serra, O. 1986, Fundamentals of well-log interpretation volume 2 - The interpretation of logging data: Developments in Petroleum Science No. 15B, Elsevier, Amsterdam, 684 p.

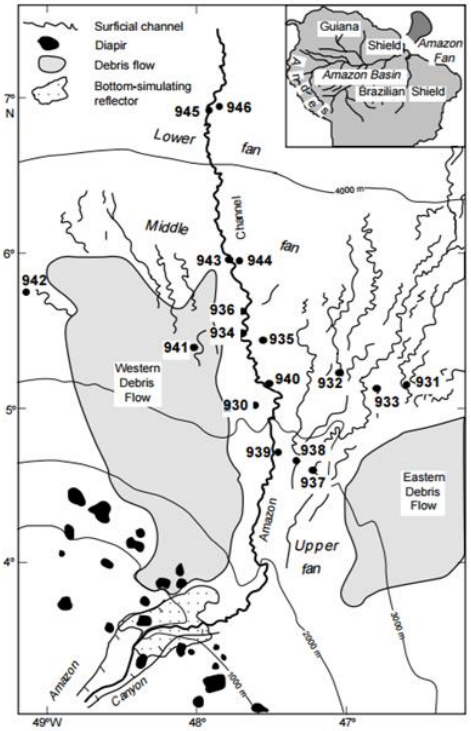

Figure 1. Morphological features and physiographic limits of the Amazonian River Fan. It is possible to observe the Amazon Canyon in the upper part of the fan, followed by the middle and lower portions (modified from Oliveira, 2005).

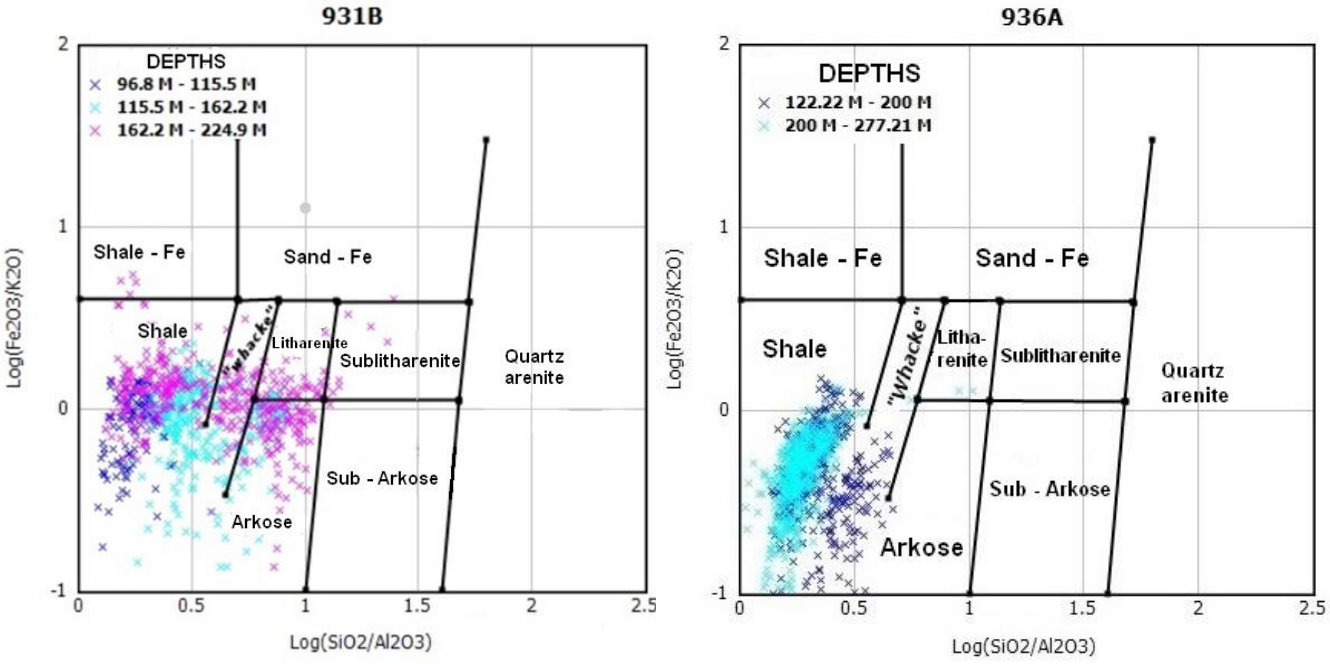

Figure 2. Classifications of the rocks by the response of the GLT log in wells 931B and 936A in accord to Herron (1988).

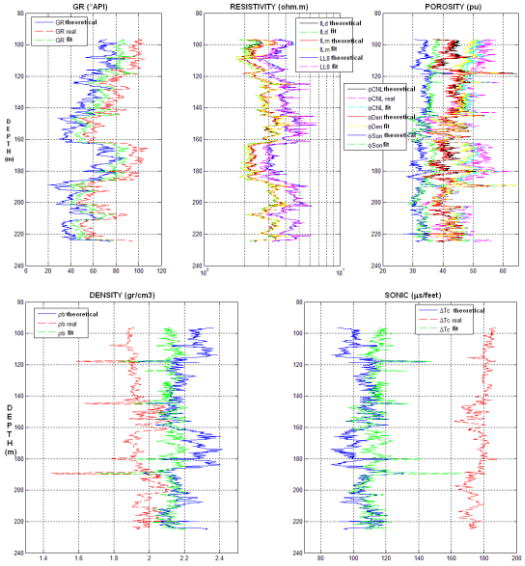

Figure 3. Actual and adjusted theoretical responses of the gamma ray, resistivity, porosity, density and sonic logs for well 931B.

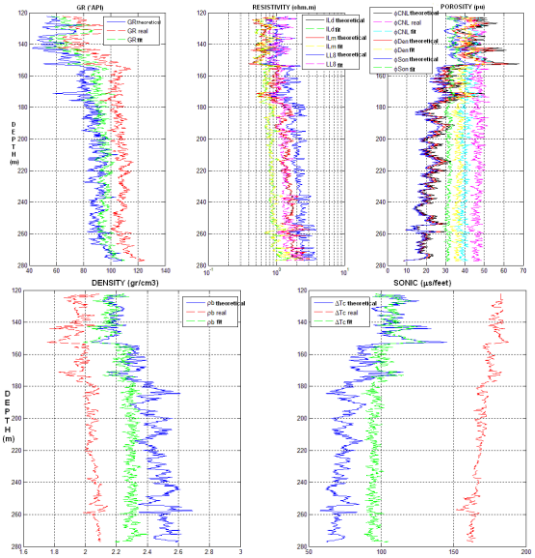

Figure 5. Actual and adjusted theoretical responses of the gamma ray, resistivity, porosity, density and sonic logs for well 936A.

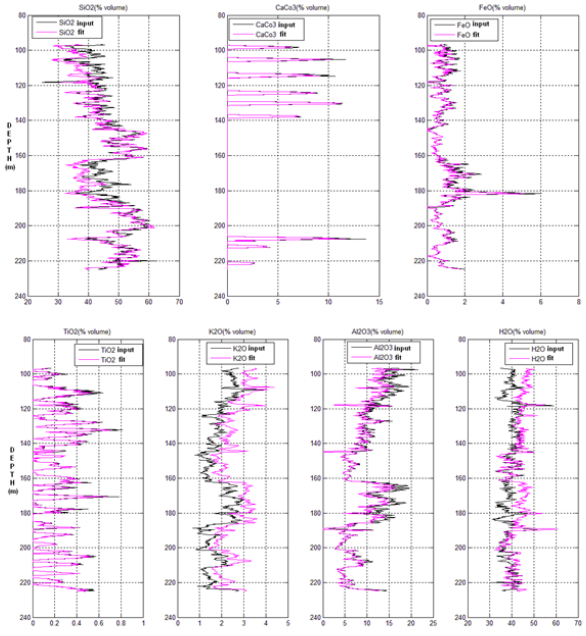

Figure 4. Input and fit values of the mineral oxides (SiO2, CaCO3 and FeOTiO2, K2O and Al2O3) and H2O for well 931B.

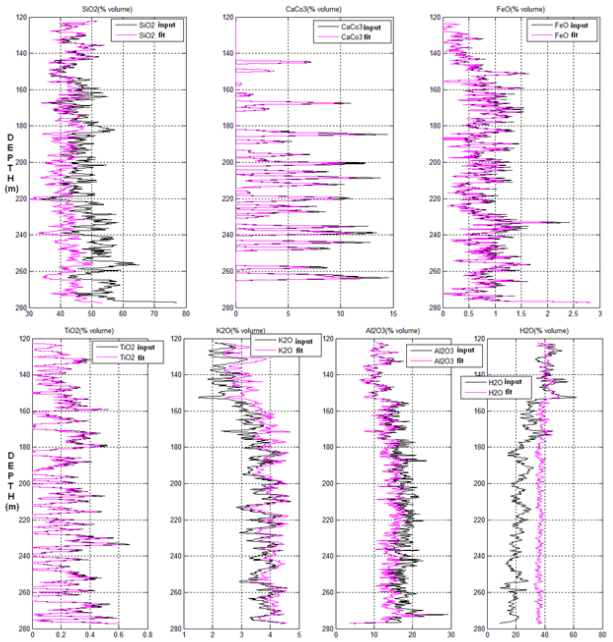

Figure 6. Input and adjustment values of the mineral oxides (SiO2, CaCO3 and FeOTiO2, K2O and Al2O3) and H2O for well 936A.